3D Spin-Liquid State in an Organic Hyperkagome Lattice of Mott Dimers

Asato Mizuno,[1] Yoshiaki Shuku,[2] Michio M. Matsushita,[1] Masahisa Tsuchiizu,[3] Yuuki Hara,[3] Nobuo Wada,[3]
Yasuhiro Shimizu,[3] and Kunio Awaga[1]
[1]*Department of Chemistry & Integrated Research Consortium on Chemical Sciences (IRCCS), Nagoya University,*
Furo-cho, Chikusa-ku, Nagoya 464-8602, Japan
[2]*Venture business laboratory (VBL), Nagoya University, Furo-cho, Chikusa-ku, Nagoya 464-8602, Japan*
[3]*Department of Physics, Nagoya University, Furo-cho, Chikusa-ku, Nagoya 464-8602, Japan*

(Received 17 December 2016; revised manuscript received 5 April 2017; published 31 July 2017)

We report the first 3D spin liquid state of isotropic organic spins. Structural analysis, and magnetic and heat–capacity measurements were carried out for a chiral organic radical salt, $(\mathrm{TBA})_{1.5}[(-)\text{-NDI-}\Delta]$ (TBA denotes tetrabutylammonium and NDI denotes naphthalene diimide), in which $(-)$-NDI-Δ forms a K_4 structure due to its triangular molecular structure and an intermolecular π-π overlap between the NDI moieties. This lattice was identical to the hyperkagome lattice of $S = 1/2$ Mott dimers, and should exhibit 3D spin frustration. In fact, even though the high-temperature magnetic susceptibility followed the Curie-Weiss law with a negative Weiss constant of $\theta = -15$ K, the low-temperature magnetic measurements revealed no long-range magnetic ordering down to 70 mK, and suggested the presence of a spin liquid state with a large residual paramagnetism χ_0 of 8.5×10^{-6} emu g^{-1} at the absolute zero temperature. This was supported by the ^{14}N NMR measurements down to 0.38 K. Further, the low-temperature heat capacities c_p down to 68 mK clearly indicated the presence of c_p for the spin liquid state, which can be fitted to the power law of $T^{0.62}$ in the wide temperature range 0.07–4.5 K.

DOI: 10.1103/PhysRevLett.119.057201

Geometrical spin frustration has been investigated extensively in the past two decades [1–13], and the formation of a quantum spin liquid state, predicted by the resonating valence bond theory [14], has attracted much attention. However, most spin-frustrated systems studied thus far have been 2D triangular and kagome lattices [1–3,5–12], and thus the features of the spin frustrations in them were affected by minor factors, such as structural deformations from equilateral triangles, and interlayer interactions between the 2D lattices [8,15–17]. Furthermore, magnetic anisotropies caused by spin-orbit coupling also governed the spin ground states of the materials, which contained heavy elements such as Ni, Cu, and Ir [4,18,19]. From this perspective, it is preferable to elucidate 3D spin-frustrated systems of an $S = 1/2$ Heisenberg spin, because the spin and structural isotropies of such systems can be ideal for the study of quantum spin liquids. In the present Letter, we describe a 3D spin-frustrated hyperkagome lattice of $S = 1/2$ unpaired electrons in an organic radical salt, and the formation of a spin liquid state.

In our previous work [20], we found a K_4 structure [see Fig. 1(a), Ref. [21], and the Supplemental Material [22]] in the crystal of an organic radical salt, $\mathrm{Rb}_{1.4}[(-)\text{-NDI-}\Delta]$ (NDI denotes naphthalene diimide). $(-)$-NDI-Δ [see Fig. 1(b), Ref. [34]], which consists of three NDI moieties, is a chiral triangular organic molecule. This K_4 structure is identical to the srs net, which is known as a 3D chiral network structure of regular triangles in the field of crystallography [35,36]. The K_4 structure is also isostructural to the gyroid or G-surface structure [37,38], which is an infinitely connected 3D-periodic minimal surface, mathematically discovered by Schoen [39]. In the crystals of $\mathrm{Rb}_{1.4}[(-)\text{-NDI-}\Delta]$ [see Fig. 1(c)], the

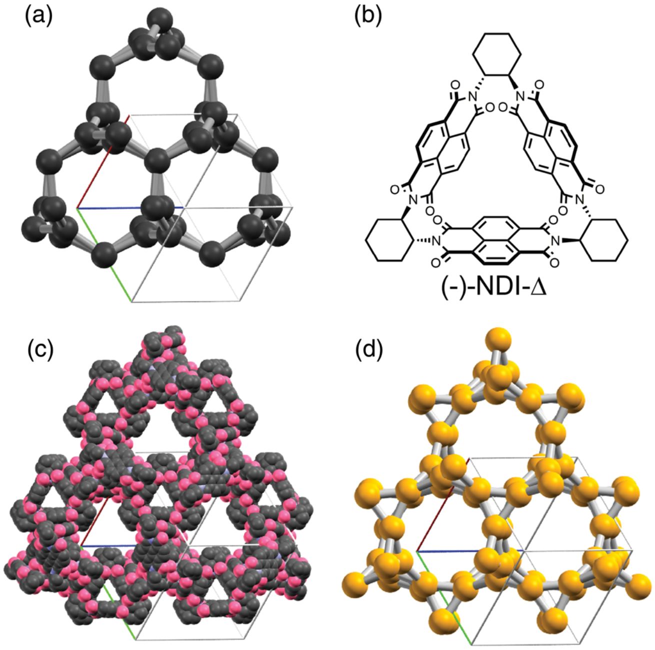

FIG. 1. Comparison of the structures of the K_4 carbon (a), the molecular structure of $(-)$-NDI-Δ (b), the K_4 structure of $(-)$-NDI-Δ (c), and the hyperkagome lattice, formed by the unpaired electrons on the Mott dimers (d).

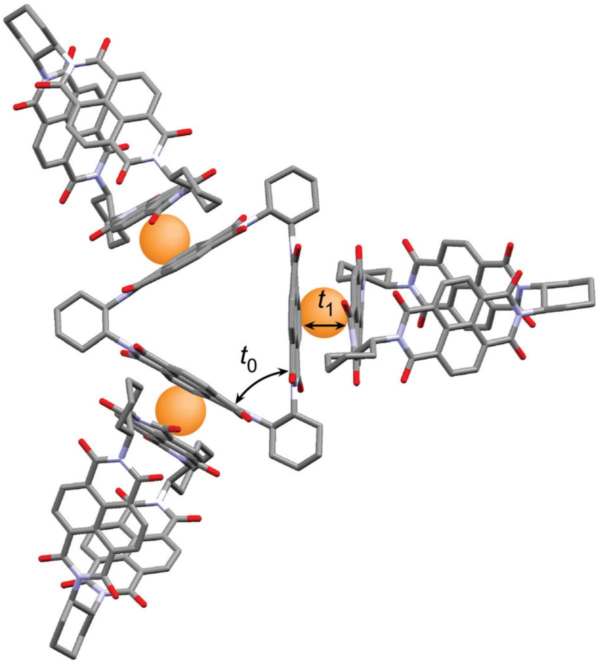

FIG. 2. Nearest-neighbor intermolecular arrangements of the (−)-NDI-Δ anion radicals in the TBA salt. The parameters, t_0 and t_1, indicate the intra- and intermolecular transfer integrals, respectively. The orange circles indicate the locations of the $S = 1/2$ unpaired electrons.

(−)-NDI-Δ anion radicals form the K_4 structure by the three-way branched, intermolecular π-π overlaps (see Fig. 2) [20]. Since the valence of (−)-NDI-Δ in $Rb_{1.4}$[(−)-NDI-Δ] included an ambiguity, namely, -1.4 ± 0.1 due to occupational disorder of Rb^+ ions, we prepared an isostructural salt, $(TBA)_{1.5}$[(−)-NDI-Δ] (TBA denotes tetrabutylammonium) with no ambiguity in the chemical stoichiometry, in order to elucidate the low temperature physics in detail.

We prepared the chiral molecule, (−)-NDI-Δ, according to the literature method [34] and obtained black block chiral crystals of $(TBA)_{1.5}$[(−)-NDI-Δ] by galvanostatic electrocrystallization in diglyme with TBA·ClO_4. X-ray analysis revealed the K_4 structure of (−)-NDI-Δ in this crystal [see Fig. 1(c)], while it belonged to the cubic space group of $P4_332$ instead of $I4_132$ for $Rb_{1.4}$[(−)-NDI-Δ]. This disagreement owes not to a difference between the K_4 structures of (−)-NDI-Δ in the two salts, but rather to the positions of the Rb^+ and TBA^+ ions in them (see Fig. S2 [22]). In $(TBA)_{1.5}$[(−)-NDI-Δ], the structures and positions of the TBA^+ ions were successfully refined with the occupation number of 1. It was found that one TBA^+ ion is shared by two neighboring (−)-NDI-Δ molecules, so that the ratio of TBA to (−)-NDI-Δ is 1.5:1. The valence of (−)-NDI-Δ was determined as −1.5 without ambiguity. The IR spectra of the two salts also indicated that the (−)-NDI-Δ molecules in them have nearly the same valence (see Fig. S3 [22]). Figure S4 shows a room-temperature EPR signal of $(TBA)_{1.5}$[(−)-NDI-Δ] (polycrystalline samples) and the temperature dependence of the g factor down to 5 K. Since (−)-NDI-Δ consists of only the light elements, C, H, N, and O, the g factor (=2.0036) is close to that of free electron in the whole measurement range. This means that the spins on the (−)-NDI-Δ anion radicals would be regarded as isotropic Heisenberg spins.

On the basis of the crystal structure, we calculated the intra- and intermolecular transfer integrals as $t_0 = -0.034$ and $t_1 = -0.27$ eV, respectively (see Fig. 2 and Table S2 [22]). The latter is an order of magnitude larger than the former. We then determined the band structure of $(TBA)_{1.5}$[(−)-NDI-Δ], as shown in Fig. S6 [22]. This indicated a metallic ground state and very exotic features, such as 3D Dirac cones and degenerate flat bands, which were essentially the same as those for $Rb_{1.4}$[(−)-NDI-Δ] [20,40–43]. In spite of this calculation, we confirmed the insulating ground state of $(TBA)_{1.5}$[(−)-NDI-Δ] and $Rb_{1.4}$[(−)-NDI-Δ], by using the two-probe method to measure the temperature dependence of the conductivity (see Fig. S7 [22]).

Let us discuss the spin lattice, formed in the K_4 structure of $(TBA)_{1.5}$[(−)-NDI-Δ]. One (−)-NDI-Δ bears a −1.5 charge, so that a half electron exists on the NDI unit, which is one-third of (−)-NDI-Δ. Since the intermolecular interaction is much stronger than the intramolecular one, it is reasonable to conclude that one unpaired electron is held by the intermolecular NDI dimer unit (see Fig. 2). The positions of the TBA^+ ions also support this interpretation. Further, since $(TBA)_{1.5}$[(−)-NDI-Δ] is an insulator, it is also expected that the weak intramolecular interaction t_0, corresponding to the interaction between the unpaired electrons, would result in the localization of the unpaired electrons. These features closely resemble those of the Mott dimer systems found in the organic radical salts of bis(ethylenedithia)tetrathiafulvalene (BEDT-TTF) [44,45]. In these materials, one BEDT-TTF dimer unit bears one unpaired electron, and these dimer units form a triangular lattice with spin frustration. By transforming the K_4 lattice of (−)-NDI-Δ into a lattice of unpaired electrons, we have found that the spin lattice corresponds to a so-called hyperkagome lattice, consisting of corner-sharing triangles [see Fig. 1(d) and a movie in the Supplemental Material [22]]. This is the first example of an organic hyperkagome lattice with isotropic $S = 1/2$ spins.

The temperature dependence of the magnetic susceptibility of $(TBA)_{1.5}$[(−)-NDI-Δ] was measured in the range between 2 and 300 K on a SQUID susceptometer (a Quantum Design Magnetic Property Measurement System MPMS-XL magnetometer). After the diamagnetic corrections, we obtained the paramagnetic susceptibility, χ_p. The results are shown in Fig. S8 [22]. The high-temperature data can be fitted to the Curie-Weiss law, with a Curie constant of $C = 2.1 \times 10^{-4}$ emu K g^{-1} and a Weiss constant of $\theta = -15$ K. This negative Weiss constant indicates an antiferromagnetic interaction among the unpaired electrons, and agrees roughly with the corresponding thermal energy of t_0. This interaction is expected to induce a spin frustration on the hyperkagome lattice of the Mott dimers.

We measured low-temperature magnetic susceptibility from 6 K to 70 mK by using a homemade SQUID susceptometer mounted on a dilution refrigerator [22]. By smoothly connecting these low-temperature data and the high-temperature χ_p above 2 K in Fig. S8 [22], we obtained the temperature dependence of χ_p in the whole range of 0.07–300 K. The results are shown as log χ_p vs log T plots in Fig. 3(a). As the temperature decreases from 300 K, χ_p increases monotonically. After passing through a small anomaly around 20 K, which is probably caused by a short-range magnetic interaction due to t_0, χ_p continues to increase down to the lowest temperature. The data indicate no long-range magnetic ordering in spite of the 3D antiferromagnetic interactions with $\theta = -15$ K. The temperature dependence of ^{14}N NMR of $(\mathrm{TBA})_{1.5}[(-)\text{-NDI-}\Delta]$ was examined in the range between 0.38 and 150 K by measuring spin-echo spectra at a constant magnetic field of 8.71 T. Figure 3(b) shows the spectra at representative temperatures. The NMR signal shapes are governed by nuclear quadrupole interactions for the nuclear spin $^{14}I = 1$. It is clearly demonstrated that, though the NMR signal shapes become slightly broader with a decrease in temperature, there is no drastic change such as is seen in long-range magnetic ordering. It is notable that this type of small linewidth broadening was recognized in the spin liquid states of κ-$(\mathrm{BEDT\text{-}TTF})_2\mathrm{Cu}_2(\mathrm{CN})_3$ [11] and $\mathrm{EtMe_3Sb[Pd(dmit)_2]_2}$ (Et, Me, and dmit denote ethyl, methyl, and 1,3-dithiole-2-thione-4,5-dithiolate, respectively) [12]. These magnetic data strongly suggest the presence of spin frustration on the hyperkagome lattice and the formation of a spin liquid state, instead of magnetic ordering.

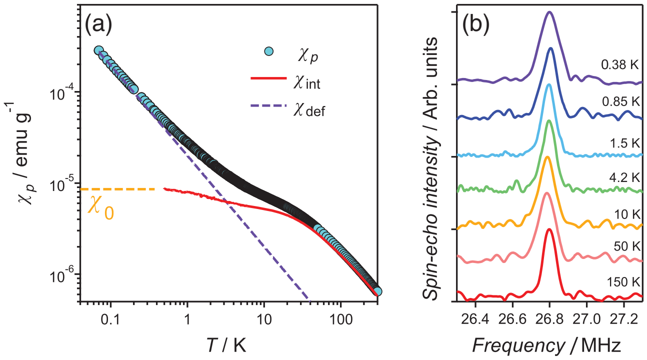

FIG. 3. (a) Temperature dependence of paramagnetic susceptibility χ_p in the temperature range 0.07–300 K for $(\mathrm{TBA})_{1.5}[(-)\text{-NDI-}\Delta]$. The purple broken line and the red curve indicate those of χ_{def} and χ_{int}, respectively. See the text. (b) Temperature dependence of ^{14}N NMR signals for $(\mathrm{TBA})_{1.5}[(-)\text{-NDI-}\Delta]$ at representative temperatures in the range 0.38–150 K.

The temperature dependence of the heat capacity c_p of $(\mathrm{TBA})_{1.5}[(-)\text{-NDI-}\Delta]$ was measured in the temperature ranges 2–50 K and 0.068–4.5 K on a Quantum Design Physical Property Measurement System (PPMS) and a homemade calorimeter mounted on a dilution refrigerator, respectively [22]. The former was calibrated before the measurements by using a copper standard sample [22]. Figure 4(a) shows the temperature dependence of c_p in the whole temperature range; the values of c_p gradually decrease as the temperature decreases, and begins to increase very slightly below 0.1 K. This is also consistent with the absence of long-range magnetic ordering. To estimate the lattice contribution, the heat capacity data below 5 K are replotted as c_p/T vs T^2 in Fig. S9. With a

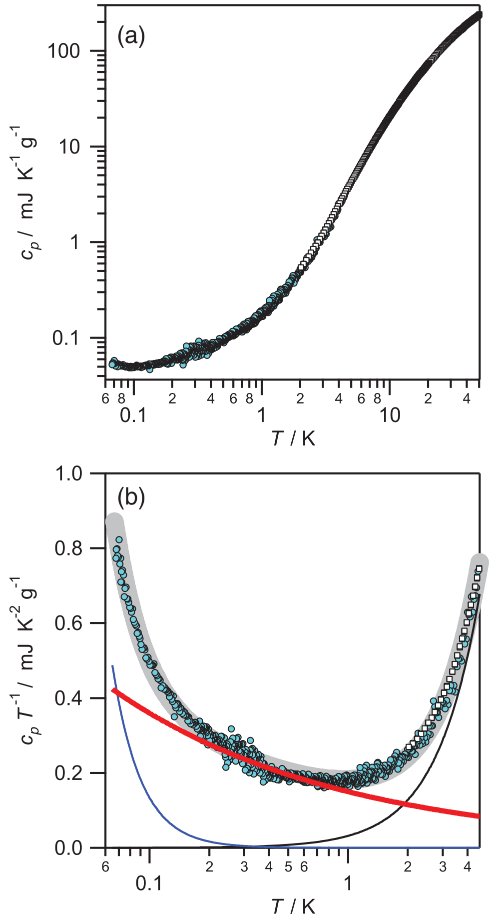

FIG. 4. Temperature dependence of heat capacity c_p for $(\mathrm{TBA})_{1.5}[(-)\text{-NDI-}\Delta]$ in the plots of log c_p vs log T in the range 0.068–50 K (a) and c_p/T vs log T in the range 0.068–5 K (b). The open squares and the blue circles indicate the data, taken on a PPMS and a homemade calorimeter, respectively. The blue, bold red, and black curves indicate the contributions of the first, second, and third terms in the equation $c_p = aT^{-2} + bT^{\xi} + \beta T^3$, respectively.

decrease in temperature, the values of c_p/T show a linear decrease, followed by a sudden increase below ca. 0.1 K. Such an increase at very low temperatures has been often observed in organic spin systems, and has been attributed to a high-temperature tail of a Schottky peak, formed by nuclear spins, weak magnetic interactions between paramagnetic defects, or internal molecular rotations [46]. In fact, c_p is nearly proportional to T^{-2} at the lowest temperatures, as shown in the next section. Above 1 K, there is a linear relation between c_p/T and T^2 with a lattice capacity coefficient of $\beta = 0.028\ \mathrm{mJ\,K^{-4}\,g^{-1}}$. The extrapolation of this line to the absolute zero temperature, clearly reaches a nonzero value, which means the presence of a large heat capacity for the spin liquid state.

We performed a detailed analysis on the heat capacity data, to estimate the intrinsic temperature dependence of c_p for the spin liquid state. Figure 4(b) shows the plots of c_p/T vs $\log T$ below 5 K, in which the increases in c_p/T at the high- and low-temperature sides are the lattice contribution and the high-temperature tail of the Schottky anomaly, respectively. It was found that this temperature dependence can be well explained by the equation, $c_p = aT^{-2} + bT^{\xi} + \beta T^3$, where the first term is for the contribution of the Schottky tail below 0.1 K, the second term is for the spin liquid state, and the third term is for the lattice contribution above 1 K. By optimizing the values of a, b, and ξ, we obtained the theoretical best fit with $\xi = 0.62$, as shown by the bold gray curve in Fig. 4(b). The blue, bold red, and black curves indicate the contributions of the first, second, and third terms, respectively. It is worth noting that, without adding the second term, we could not obtain any reasonable fitting. The contributions of the first and third terms are negligibly small in the temperature range between 0.2 and 0.6 K, so that the agreement between the experimental plots and the theoretical curve in this temperature range, strongly justify that c_p is proportional to $T^{0.62}$ in the spin liquid state. It is reported that the temperature dependence of c_p exhibits a T^2 term in the inorganic 3D hyperkagome systems such as $\mathrm{Na_4Ir_3O_8}$ [4], though a simple comparison with the present organic system does not make sense, because these inorganic systems involve strong magnetic interactions and magnetic anisotropies caused by spin-orbit interactions. The low-temperature heat capacities near the quantum critical points in the 2D and 3D systems are theoretically predicted to exhibit $T^{2/3}$ and $T\ln(1/T)$ dependences, respectively, in the context of the heavy-fermion problem [47], but we could not obtain any reasonable fitting with a $T\ln(1/T)$ term, instead of the T^{ξ} term. It is not certain whether the fairly good agreement between the observed T^{ξ} behavior and the $T^{2/3}$ dependence for the 2D system is meaningful or not. In any case, the theoretical understanding of the present hyperkagome system of organic Heisenberg spins will be a future challenge.

We briefly mention the frustration parameter and the Wilson ratio, since these parameters have been discussed for spin liquid systems in the literature [1,9,48]. The frustration parameter [1,49] can be easily calculated as $|\theta/T_N| > 200$, which is large enough for spin frustration. By the procedure in the Supplemental Material [22], we roughly estimated the χ_0 value ($=8.5 \times 10^{-6}\ \mathrm{emu\,g^{-1}}$), which is the extrapolation of the intrinsic paramagnetic susceptibility to the absolute zero temperature. This reflects gapless magnetic excitations of the spin liquid states. In Fig. 3(a), the purple broken line shows the temperature dependence of the paramagnetic susceptibility caused by lattice defect χ_{def}, and the red curve shows the intrinsic paramagnetic susceptibility χ_{int}, calculated by $\chi_{\mathrm{int}} = \chi_p - \chi_{\mathrm{def}}$. The value of χ_0 corresponds roughly to $7.9 \times 10^{-3}\ \mathrm{emu\,mol^{-1}}$ for the unit molar mass of the unpaired electrons ($\mathrm{C_{56}H_{64}N_5O_8}$ with molecular mass $= 935$), and is an order of magnitude larger than those for the other organic triangular systems, namely, $\chi_0 = 2.9\times10^{-4}\,\mathrm{emu\,mol^{-1}}$ for κ-$\mathrm{(BEDT\text{-}TTF)_2Cu_2(CN)_3}$ [11] and $\chi_0 = 4.4 \times 10^{-4}\ \mathrm{emu\,mol^{-1}}$ for $\mathrm{EtMe_3Sb[Pd(dmit)_2]_2}$ [12]. Although we concluded $T^{0.62}$ dependence of c_p, we calculated the value of c_p/T at $T = 1$ K ($=0.15\ \mathrm{mJ\,K^{-2}\,g^{-1}}$) as a parameter which corresponds to the electronic capacity coefficient γ. This value is converted roughly to $1.4 \times 10^2\ \mathrm{mJ\,K^{-2}\,mol^{-1}}$, and is an order of magnitude larger than those of the other organic triangular systems, namely, $\gamma = 12\ \mathrm{mJ\,K^{-2}\,mol^{-1}}$ for κ-$\mathrm{(BEDT\text{-}TTF)_2Cu_2(CN)_3}$ [50] and $\gamma = 19.9\ \mathrm{mJ\,K^{-2}\,mol^{-1}}$ for $\mathrm{EtMe_3Sb[Pd(dmit)_2]_2}$ [48]. Then, the Wilson ratio is calculated as $R = 4.2$ for $\mathrm{(TBA)_{1.5}}$[(−)-NDI-Δ], using $R = 4\pi^2 k_B^2 \chi_0/(3g^2\mu_B^2\gamma)$ [1]. This value is in the same order of magnitude as those of the other spin liquids with weak spin-orbit coupling [1,9,48].

In summary, we solved the K_4 crystal structure of $\mathrm{(TBA)_{1.5}}$[(−)-NDI-Δ], and clearly determined the valence of (−)-NDI-Δ as −1.5. This valence determination along with the insulating ground state strongly indicated that the present system should be regarded as a Mott dimer system and that the spin structure, formed by $S = 1/2$ unpaired electrons, should correspond to a hyperkagome lattice with spin frustration. The low-temperature magnetic and thermal measurements clearly indicated the presence of a spin liquid state, with the intrinsic paramagnetism at the absolute zero temperature and $T^{0.62}$ dependence of c_p.

This work was supported by a Grant-in-Aid for Scientific Research from the Ministry of Education, Culture, Sports, Science, and Technology of Japan (MEXT). Funds were also provided by the Japan Society for the Promotion of Science (JSPS) Core-to-Core Program (A. Advanced Research Networks) and by JSPS KAKENHI Grants. A. M. acknowledges a Grant-in-Aid for the JSPS Research Fellowship program.

[1] L. Balents, Nature (London) **464**, 199 (2010).

[2] Z. Hiroi, H. Yoshida, Y. Okamoto, and M. Takigawa, J. Phys. Conf. Ser. **145**, 012002 (2009).

[3] Y. Okamoto, H. Yoshida, and Z. Hiroi, J. Phys. Soc. Jpn. **78**, 033701 (2009).

[4] Y. Okamoto, M. Nohara, H. Aruga-Katori, and H. Takagi, Phys. Rev. Lett. **99**, 137207 (2007); G. Chen and L. Balents, Phys. Rev. B **78**, 094403 (2008).

[5] K. Ishida, M. Morishita, K. Yawata, and H. Fukuyama, Phys. Rev. Lett. **79**, 3451 (1997); E. Collin, S. Triqueneaux, R. Harakaly, M. Roger, C. Bäuerle, Yu. M. Bunkov, and H. Godfrin, Phys. Rev. Lett. **86**, 2447 (2001); R. Masutomi, Y. Karaki, and H. Ishimoto, Phys. Rev. Lett. **92**, 025301 (2004).

[6] S. Nakatsuji, Y. Nambu, H. Tonomura, O. Sakai, S. Jonas, C. Broholm, H. Tsunetsugu, Y. Qiu, and Y. Maeno, Science **309**, 1697 (2005).

[7] H. D. Zhou, E. S. Choi, G. Li, L. Balicas, C. R. Wiebe, Y. Qiu, J. R. D. Copley, and J. S. Gardner, Phys. Rev. Lett. **106**, 147204 (2011).

[8] J. G. Cheng, G. Li, L. Balicas, J. S. Zhou, J. B. Goodenough, C. Xu, and H. D. Zhou, Phys. Rev. Lett. **107**, 197204 (2011).

[9] Y. Li, B. Pan, S. Li, W. Tong, L. Ling, Z. Yang, J. Wang, Z. Chen, Z. Wu, and Q. Zhang, New J. Phys. **16**, 093011 (2014).

[10] T. Isono, H. Kamo, A. Ueda, K. Takahashi, M. Kimata, H. Tajima, S. Tsuchiya, T. Terashima, S. Uji, and H. Mori, Phys. Rev. Lett. **112**, 177201 (2014).

[11] Y. Shimizu, K. Miyagawa, K. Kanoda, M. Maesato, and G. Saito, Phys. Rev. Lett. **91**, 107001 (2003).

[12] T. Itou, A. Oyamada, S. Maegawa, M. Tamura, and R. Kato, J. Phys. Condens. Matter **19**, 145247 (2007); Phys. Rev. B **77**, 104413 (2008); T. Itou, A. Oyamada, S. Maegawa, and R. Kato, Nat. Phys. **6**, 673 (2010).

[13] K. Awaga, T. Okuno, A. Yamaguchi, M. Hasegawa, T. Inabe, Y. Maruyama, and N. Wada, Phys. Rev. B **49**, 3975 (1994); N. Wada, T. Kobayashi, H. Yano, T. Okuno, A. Yamaguchi, and K. Awaga, J. Phys. Soc. Jpn. **66**, 961 (1997).

[14] P. W. Anderson, Mater. Res. Bull. **8**, 153 (1973).

[15] R. Coldea, D. A. Tennant, and Z. Tylczynski, Phys. Rev. B **68**, 134424 (2003).

[16] Y. Shirata, H. Tanaka, A. Matsuo, and K. Kindo, Phys. Rev. Lett. **108**, 057205 (2012).

[17] K. Kanoda and R. Kato, Annu. Rev. Condens. Matter Phys. **2**, 167 (2011); T. Hiramatsu, Y. Yoshida, G. Saito, A. Otsuka, H. Yamochi, M. Maesato, Y. Shimizu, H. Ito, and H. Kishida, J. Mater. Chem. C **3**, 1378 (2015).

[18] A. Zorko, S. Nellutla, J. van Tol, L. C. Brunel, F. Bert, F. Duc, J.-C. Trombe, M. A. de Vries, A. Harrison, and P. Mendels, Phys. Rev. Lett. **101**, 026405 (2008).

[19] E. Chappel, M. D. Núñez-Regueiro, G. Chouteau, O. Isnard, and C. Darie, Eur. Phys. J. B **17**, 615 (2000).

[20] A. Mizuno, Y. Shuku, R. Suizu, M. M. Matsushita, M. Tsuchiizu, D. R. Mañeru, F. Illas, V. Robert, and K. Awaga, J. Am. Chem. Soc. **137**, 7612 (2015).

[21] T. Sunada, Not. Am. Math. Soc. **55**, 208 (2008); *Topological Crystallography With a View Towards Discrete Geometric Analysis Surveys and Tutorials in the Applied Mathematical Sciences*, edited by L. Sirovich, S. Antman, M. P. Brenner, P. Holmes, L. Mahadevan, A. Singer, K. R. Sreenivasan, and J. Victor (Springer, Tokyo, 2013), Vol. 6.

[22] See Supplemental Material at http://link.aps.org/supplemental/10.1103/PhysRevLett.119.057201 for experimental details, crystallographic details, IR spectra, band calculation, magnetic data, conductivity measurements, and a movie on the hyperkagome lattice, which includes Refs. [23–33].

[23] *RAPID-AUTO Ver. 2.40* (Rigaku Corporation, Tokyo, Japan, 2006).

[24] G. M. Sheldrick, Acta Crystallogr. Sect. A **64**, 112 (2008).

[25] *CrystalStructure 4.2.2: Crystal Structure Analysis Package* (Rigaku Corporation, Tokyo, Japan, 2016).

[26] A. L. Spek, Acta Crystallogr. Sect. D **65**, 148 (2009).

[27] R. W. W. Hooft, L. H. Straver, and A. L. Spek, J. Appl. Crystallogr. **41**, 96 (2008).

[28] Y. Karaki, K. Kuga, K. Kimura, S. Nakatsuji, K. Matsubayashi, and Y. Uwatoko, J. Phys. Soc. Jpn. **84**, 084708 (2015).

[29] J. C. Lashley, M. F. Hundley, A. Migliori, J. L. Sarrao, P. G. Pagliuso, T. W. Darling, M. Jaime, J. C. Cooley, W. L. Hults, L. Morales, D. J. Thoma, J. L. Smith, J. Boerio-Goates, B. F. Woodfield, G. R. Stewart, R. A. Fisher, and N. E. Phillips, Cryogenics **43**, 369 (2003).

[30] C. A. Kennedy, M. Stancescu, R. A. Marriott, and M. A. White, Cryogenics **47**, 107 (2007).

[31] S. W. V. Sciver, *Helium Cryogenics*, 2nd ed., International Cryogenics Monograph Series edited by K. D. Timmerhaus and C. Rizzuto (Springer, New York, 2012), p. 24.

[32] T. Matsushita, N. Hori, S. Takata, N. Wada, N. Amaya, and Y. Hosokoshi, Phys. Rev. B **95**, 020408(R) (2017).

[33] M. J. Frisch *et al.*, *Gaussian 09, Revision E.01* (Gaussian, Inc., Wallingford CT, 2009).

[34] S. T. Schneebeli, M. Frasconi, Z. Liu, Y. Wu, D. M. Gardner, N. L. Strutt, C. Cheng, R. Carmieli, M. R. Wasielewski, and J. F. Stoddart, Angew. Chem., Int. Ed. **52**, 13100 (2013).

[35] M. O'Keeffe, M. A. Peskov, S. J. Ramsden, and O. M. Yaghi, Acc. Chem. Res. **41**, 1782 (2008).

[36] O. D. Friedrichs, M. O'Keeffe, and Om M. Yaghi, Acta Crystallogr. Sect. A **59**, 22 (2003).

[37] A. H. Schoen, Not. Am. Math. Soc. **55**, 663 (2008).

[38] S. T. Hyde, M. O'Keeffe, and D. M. Proserpio, Angew. Chem., Int. Ed. **47**, 7996 (2008).

[39] A. H. Schoen, NASA Technical Note, TN D-5541 (1970).

[40] M. Itoh, M. Kotani, H. Naito, T. Sunada, Y. Kawazoe, and T. Adschiri, Phys. Rev. Lett. **102**, 055703 (2009).

[41] M. Udagawa and Y. Motome, J. Phys. Conf. Ser. **145**, 012013 (2009).

[42] J. L. Mañes, Phys. Rev. B **85**, 155118 (2012).

[43] M. Tsuchiizu, Phys. Rev. B **94**, 195426 (2016).

[44] R. P. Shibaeva and E. B. Yagubskii, Chem. Rev. **104**, 5347 (2004).

[45] B. J. Powell and R. H. McKenzie, Rep. Prog. Phys. **74**, 056501 (2011).

[46] M. Sorai, S. Murakawa, T. Kotani, and H. Suga, J. Phys. Chem. Solids **44**, 1133 (1983).

[47] T. Senthil, M. Vojta, and S. Sachdev, Phys. Rev. B **69**, 035111 (2004).

[48] S. Yamashita, T. Yamamoto, Y. Nakazawa, M. Tamura, and R. Kato, Nat. Commun. **2**, 275 (2011).

[49] A. P. Ramirez, Annu. Rev. Mater. Sci. **24**, 453 (1994).

[50] S. Yamashita, Y. Nakazawa, M. Oguni, Y. Oshima, H. Nojiri, Y Shimizu, K. Miyagawa, and K. Kanoda, Nat. Phys. **4**, 459 (2008).